ELSEVIER

Journal of Fluids and Structures 21 (2005) 609–627

JOURNAL OF FLUIDS AND STRUCTURES

www.elsevier.com/locate/jfs

A nonlinear model for an extensible slender flexible cylinder subjected to axial flow

Y. Modarres-Sadeghi*, M.P. Païdoussis, C. Semler

Department of Mechanical Engineering, McGill University, Montreal, QC, Canada H3A 2K6

Received 9 June 2004; accepted 24 February 2005

Abstract

In this paper, the weakly nonlinear equations of motion are derived for a slender flexible cylinder subjected to axial flow. The cylinder centreline is considered to be extensible, and hence two coupled nonlinear equations describe its motions, involving both longitudinal and transverse displacements. The fluid forces are formulated in terms of several components, for convenience. For high Reynolds number flows, the dominant, inviscid component is modelled by an extension of Lighthill's slender-body work; frictional, hydrostatic and pressure-loss forces are then added to the inviscid component. The derivation of the equations of motion is carried out in a Lagrangian framework, and the resultant equations are correct to third-order of magnitude, $\mathcal{O}(\varepsilon^3)$, where the transverse displacement of the cylinder is of $\mathcal{O}(\varepsilon)$. This is the main contribution of this paper; however, the equations have been solved and some interesting results are presented also. Bifurcation diagrams with flow velocity as the independent variable, supported by phase-plane plots, show that the system loses stability via a supercritical pitchfork bifurcation and develops divergence, and at higher flow flutter, which is what has been observed experimentally and predicted by linear theory in the past. It is shown that post-divergence flutter does exist, not as an instability of the trivial equilibrium (as predicted by linear theory), but as a Hopf bifurcation emanating from the nonlinear static equilibrium. For high enough flow, interesting dynamics follow, including quasiperiodicity and chaos.

1. Introduction

Historically, the first specific study on the dynamics of a slender flexible cylinder subjected to axial flow was by Hawthorne (1961) and was concerned with the stability of the Dracone barge. The Dracone is a long flexible towed tubular container with tapering ends, which has been designed to carry oil and other liquids lighter than sea-water. This analysis was extended and generalized for cylinders with any boundary conditions and supported by experiments by Païdoussis (1966a, b), as well as for towed cylinders (Païdoussis, 1968). Later, a more general, corrected linear equation of motion was derived by Païdoussis (1970, 1973), and the theory was further extended to deal with cases of confined flow. The dynamics of long, very slender cylinders—modelled as strings, rather than beams—has been studied by Triantafyllou and Chryssostomidis (1985). Also, the dynamics of clustered cylinders in axial flow has been extensively studied [by Chen (1975) and Païdoussis and Suss (1977) among others; see Païdoussis (2003)], both because of its

*Corresponding author.
E-mail address: yahya.modarres-sadeghi@mcgill.ca (Y. Modarres-Sadeghi).

0889-9746/$ - see front matter © 2005 Elsevier Ltd. All rights reserved.
doi:10.1016/j.jfluidstructs.2005.02.012

inherent interest and for applications, to tube-in-shell type heat exchangers for example. Also, additional extensions to the theory have been made to deal with the dynamics in highly confined annular flow [e.g., by Païdoussis et al. (1990)]. It should be remarked that the dynamics of towed cylinders is of interest not only for the Dracone problem, but also for the towed arrays used in oil exploration. Apart from Hawthorne's and Païdoussis' original work, studies on towed systems were made by Dowling (1988a, b) and many others; see, e.g., Païdoussis (2003).

The dynamics of cylinders in axial flow is dynamically similar to that of axially moving 1-D structures in quiescent fluid, such as paper web in paper-making, and travelling chains, bands and tapes (Mote, 1968; Pramila, 1987). The dynamics of this system is also closely related to that of pipes conveying fluid (Païdoussis, 1998, 2003).

Recently, the dynamics of cantilevered flexible cylinders in axial flow has been re-examined via a nonlinear theory for the first time (Païdoussis et al., 2002; Lopes et al., 2002; Semler et al., 2002), using the centreline-inextensibility assumption, which is reasonable only for cantilevered cylinders. In that three-part study, the physical dynamics, the derivation of the nonlinear equation of motion, and the nonlinear dynamics of cantilevered cylinders in axial flow have been discussed in detail.

In this paper, a weakly nonlinear equation of motion for an extensible slender flexible cylinder subjected to axial flow, exact to third-order of magnitude, is derived, which in the linear limit is identical to that obtained by Païdoussis (1973).

2. Definitions and preliminaries

2.1. Basic assumptions and concepts

The system under consideration consists of a cylinder of length L, cross-sectional area A, mass per unit length m, and flexural rigidity EI, centrally located in a rigid channel within which a fluid flows with velocity U parallel to the channel centreline. The undeformed cylinder axis coincides with the X-axis (in the direction of gravity) and the cylinder is assumed to oscillate in the (X, Y) plane (see Fig. 1).

The basic assumptions made for the cylinder and the fluid are as follows: (i) the fluid is incompressible; (ii) the mean flow velocity is constant; (iii) the cylinder is slender, so that the Euler–Bernoulli beam theory is applicable; (iv) although the deflections of the cylinder may be large, the strains are small; (v) the cylinder centreline is extensible.

The derivation to be presented here, so far as the fluid dynamics of the system is concerned, is similar in spirit and procedure to that of Païdoussis (1966, 1973). Thus, for convenience, the inviscid, viscous and hydrostatic forces are determined separately, rather than being determined together, say by direct application of the Navier–Stokes equations.

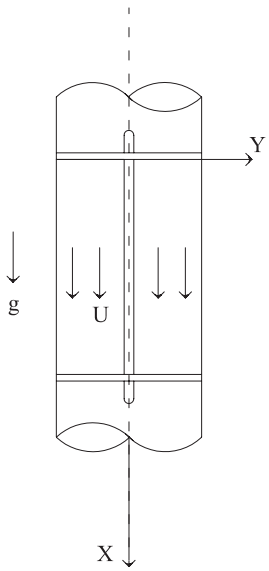

Fig. 1. Diagrammatic view of a vertical slender flexible and extensible cylinder subjected to axial flow, in the test-section of a circulation system.

2.2. Notation and coordinate systems

One usually has the choice between two sets of coordinate systems: one for the undeformed body (Lagrangian coordinates) and the other for the deformed body (Eulerian coordinates). The deformation of a point is described by the relation of the coordinates of the same material point in the undeformed and deformed states. Let (X, Y, Z) represent the position of a material point P in its original state, and (x, y, z) the position of the same point in the deformed state. Then, the displacement of that material point is defined as $u = x - X$, $v = y - Y$ and $w = z - Z$. For a slender cylinder with its initially undeformed state along the X-axis and undergoing motions in the (X, Y) plane, we have $Y = 0$, hence $y = v$; and $w = z = Z = 0$.

Defining ε as the axial strain along the centreline of the cylinder, one may relate δX and δs, where s is the curvilinear coordinate along the cylinder, through the condition

$$\varepsilon = \frac{\delta s - \delta X}{\delta X}, \tag{1}$$

and therefore

$$\varepsilon(X) = \sqrt{(1+u')^2 + v'^2} - 1, \tag{2}$$

where $(\,)' = \partial(\,)/\partial X$.

Let θ_1 be the angle between the centreline of the cylinder and the X-axis (see Fig. 2). For a cylinder undergoing planar motion, extensible or inextensible, the curvature is given by

$$\kappa = \frac{\partial \theta_1}{\partial s}. \tag{3}$$

For an extensible cylinder, θ_1 is defined via

$$\cos\theta_1 = \frac{\delta x}{\delta s} = \frac{\partial x/\partial X}{\partial s/\partial X} = \frac{\partial x/\partial X}{1+\varepsilon}, \tag{4}$$

$$\sin\theta_1 = \frac{\delta y}{\delta s} = \frac{\partial y/\partial X}{\partial s/\partial X} = \frac{\partial y/\partial X}{1+\varepsilon}. \tag{5}$$

In terms of the X-coordinate, Eq. (3) becomes

$$\kappa = \frac{\partial \theta_1}{\partial X}\frac{\partial X}{\partial s} = \frac{1}{1+\varepsilon}\frac{\partial \theta_1}{\partial X}. \tag{6}$$

Then, using (4) and (5), one can find

$$\theta_1' \equiv \frac{\partial \theta_1}{\partial X} = \frac{y''x' - y'x''}{(1+\varepsilon)^2}, \tag{7}$$

thus yielding the curvature for cylinders with an extensible centreline, namely

$$\kappa = \frac{y''x' - y'x''}{(1+\varepsilon)^3}. \tag{8}$$

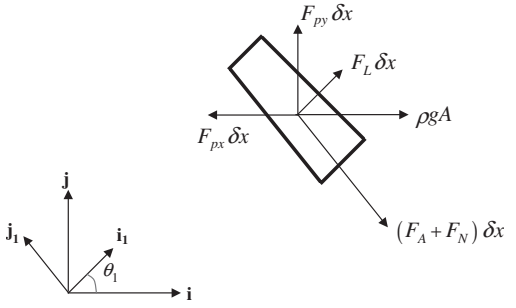

Fig. 2. An element δx of the cylinder, showing the forces acting on it.

2.3. On the derivation of the nonlinear equations of motion

Large motions imply that terms of higher order than the linear ones have to be kept in the equation; here, only quadratic and cubic nonlinear terms are retained. For planar motions, the lateral displacement may be supposed to be small, relative to the length of the cylinder, i.e., $y = v \sim \mathcal{O}(\varepsilon)$, where $\mathcal{O}(\varepsilon)$ denotes the first order. One can see that the longitudinal displacement u is one order higher than v, i.e., $u \sim \mathcal{O}(\varepsilon^2)$.

Because we have assumed that the cylinder is extensible, no relation between the virtual displacements δX and δY exists. Therefore, two equations of motion are necessary: one in the X- and the other in the Y-direction.

To derive the equations of motion we shall use Hamilton's principle, usually written as

$$\delta \int_{t_1}^{t_2} L \, \mathrm{d}t + \int_{t_1}^{t_2} \delta W \, \mathrm{d}t = 0, \tag{9}$$

where $L = T - V$ is the Lagrangian of the system, in which T and V are, respectively, the kinetic and potential energy associated with the cylinder, and δW is the virtual work due to the forces acting on the cylinder; δ is the variational operator. This variational technique requires that the quantities involved be correct to one order higher than that sought: in this case to $\mathcal{O}(\varepsilon^4)$ at least.

3. Kinetic and potential energies of cylinder

The kinetic energy of the cylinder is defined by

$$T = \frac{1}{2} m \int_0^L V_c^2 \, \mathrm{d}X = \frac{1}{2} m \int_0^L (\dot{u}^2 + \dot{v}^2) \, \mathrm{d}X, \tag{10}$$

and hence the variation of the kinetic energy is given by

$$\delta \int_{t_1}^{t_2} T \, \mathrm{d}t = -m \iint (\ddot{u}\delta u + \ddot{v}\delta v) \, \mathrm{d}X \, \mathrm{d}t, \tag{11}$$

where $\dot{(\,)} = \partial(\,)/\partial t$.

The potential energy of the cylinder comprises gravitational and strain energy components. In general, the gravitational energy depends on the distribution of mass, and is written as $V_G = \int \rho \, \phi(\xi) \, \mathrm{d}V$, where ϕ is the gravitational potential per unit mass. In a uniform gravitational field as for the system at hand, it becomes

$$V_G = -mg \int_0^L (X + u) \, \mathrm{d}X, \tag{12}$$

hence

$$\delta \int_{t_1}^{t_2} V_G \, \mathrm{d}t = -mg \iint \delta u \, \mathrm{d}X \, \mathrm{d}t. \tag{13}$$

An exact form of the strain energy, in the case of large deflections and correct to $\mathcal{O}(\varepsilon^4)$, was obtained by Stoker (1968) with only one major assumption: the strain is small, even though the deflection may be large. Stoker's analysis finally leads to

$$V_S = \frac{1}{2} E \int_0^L \left[A\varepsilon^2 + I \, (1 + \varepsilon)^2 \kappa^2 \right] \mathrm{d}X, \tag{14}$$

where X represents the Lagrangian coordinate, A the cross-sectional area, I the area-moment of inertia, and ε the axial strain.

The axial strain may itself be decomposed into two components: (i) a steady-state strain due to a tension T externally applied or associated with gravity and friction, and (ii) a time-varying strain due to cylinder oscillation. By reference to Eq. (14) and using Eq. (6), this strain energy may be expressed as

$$V_S = \frac{1}{2} EA \int_0^L \left(\frac{T}{EA} + \varepsilon \right)^2 \mathrm{d}X + \frac{1}{2} EI \int_0^L \left(\frac{\partial \theta_1}{\partial X} \right)^2 \mathrm{d}X. \tag{15}$$

Following Païdoussis (1973), the tension T can be expressed as

$$\frac{\partial T}{\partial x} = -\left(\frac{1}{2}\rho D U^2 C_T + mg\right); \tag{16}$$

then, using $\partial T/\partial X = (\partial T/\partial x)(\partial x/\partial X) = (\partial T/\partial x)(1+u')$ and integrating the resulting equation from X to L, one can find

$$T(X) = \left(\frac{1}{2}\rho D U^2 C_T + mg\right)\left[L - X + u(L)(1-\overline{\delta}) - u\right] + T(L), \tag{17}$$

where $T(L)$ is the tension at the downstream end, which can be written as

$$T(L) = \overline{T}\,\overline{\delta} + \frac{1}{2}\rho D^2 U^2 C_b(1-\overline{\delta}) - \left[\frac{1}{2}\rho D U^2 C_T\left(1+\frac{D}{D_h}\right) + mg\right]\frac{L}{2}\overline{\delta}; \tag{18}$$

$\overline{T}$ is an externally imposed uniform tension and C_b is a base pressure coefficient, in case the downstream end of the cylinder is exposed to the flow and free to slide axially (Païdoussis, 1973); $\overline{\delta}$ in Eqs. (17) and (18) is an index: $\overline{\delta}=0$ signifies that the downstream end is free to slide axially, and $\overline{\delta}=1$ if the supports do not allow net axial extension.

Therefore, the final form of the tension force becomes

$$\begin{aligned} T(X) = {} & \left(\frac{1}{2}\rho D U^2 C_T + mg\right)\left[L\left(1-\frac{1}{2}\overline{\delta}\right) - X + u(L)(1-\overline{\delta}) - u\right] \\ & - \frac{1}{2}\rho D U^2 C_T \frac{D}{D_h}\frac{L}{2}\overline{\delta} + \frac{1}{2}\rho D^2 U^2 C_b(1-\overline{\delta}) + \overline{T}\,\overline{\delta}, \end{aligned} \tag{19}$$

where it is obvious that when $\overline{\delta}=1$, $u(L)=0$.

Recalling that $u \sim \mathcal{O}(\varepsilon^2)$ and $v \sim \mathcal{O}(\varepsilon)$, and using Eqs. (2) and (7) one may obtain

$$\left(\frac{\partial \theta_1}{\partial X}\right)^2 = v''^2 - 2v''^2u' - 2v''^2v'^2 - 2v'v''u'' + \mathcal{O}(\varepsilon^5). \tag{20}$$

Therefore, using Eqs. (15), (19) and (20), we obtain

$$\begin{aligned} \delta\int_{t_1}^{t_2} V_S\,\mathrm{d}t = {} & \iint\Big\{ -EA(u''+v'v'') - EI(v''v'''+v'v'''') \\ & + \left[\frac{1}{2}\rho D^2U^2C_b(1-\overline{\delta}) + \left(\overline{T} - \frac{1}{2}\rho D U^2 C_T\frac{D}{D_h}\frac{L}{2}\right)\overline{\delta}\right]v'v'' \\ & + \left(mg + \frac{1}{2}\rho D U^2 C_T\right)\left[1+u' - \frac{1}{2}v'^2 + \left(L - X - \frac{L\overline{\delta}}{2}\right)v'v''\right]\Big\}\delta u\,\mathrm{d}X\,\mathrm{d}t \\ & + \iint\Big\{ -EA\left(v'u'' + v''u' + \frac{3}{2}v'^2v''\right) + EIv'''' \\ & - EI\left(3u'''v'' + 4u''v''' + 2u'v'''' + v'u'''' + 2v''^3 + 2v'^2v'''' + 8v'v''v'''\right) \\ & + \left(mg + \frac{1}{2}\rho D U^2 C_T\right)\left[v' - \frac{1}{2}v'^3 + \left(L - X - \frac{L\overline{\delta}}{2}\right)\left(-v'' + v'u'' + v''u' + \frac{3}{2}v'^2v''\right) + (u-u(L))v''\right] \\ & + \left[\frac{1}{2}\rho D^2U^2C_b(1-\overline{\delta}) + \left(\overline{T} - \frac{1}{2}\rho D U^2 C_T\frac{D}{D_h}\frac{L}{2}\right)\overline{\delta}\right] \\ & \times\left(-v'' + v'u'' + v''u' + \frac{3}{2}v'^2v''\right)\Big\}\delta v\,\mathrm{d}X\,\mathrm{d}t. \end{aligned} \tag{21}$$

4. Virtual work of the fluid forces acting on the cylinder

The fluid-related forces acting on the cylinder are: F_A, the inviscid hydrodynamic force, which acts in the transverse direction; F_N and F_L, the normal and longitudinal frictional forces; and F_{px} and F_{py}, the hydrostatic pressure forces in the x- and y-direction, respectively, as shown in Fig. 2.

4.1. Some preliminary relationships

In subsequent calculations, we define by U the axial flow velocity for the undisturbed flow; we also utilize U_f, which represents an axial flow velocity relative to an axially deforming cylinder (see Fig. 3). We can relate one to the other by the following relation (Lopes et al., 2002):

$$U_f = U\left(1 - \frac{\partial u}{\partial X}\right) + \mathcal{O}(\varepsilon^4). \tag{22}$$

Let us consider Fig. 3, showing an element δx subjected to deformation induced by the fluid. This representation enables one to define the angles required in the determination of the forces: i.e., θ_1, the angle between the longitudinal axis of the element and the X-axis

$$\theta_1 = \tan^{-1}\left[\frac{\partial y/\partial X}{\partial x/\partial X}\right], \tag{23}$$

and θ_2, the angle between the relative fluid-body velocity (see Eq. (29) further on) and the X-axis

$$\theta_2 = \tan^{-1}\left[\frac{\partial y/\partial t}{U_f - (\partial x/\partial t)}\right]. \tag{24}$$

In the definition of θ_2, we notice that the axial velocity of the cylinder is indeed taken into account. It should be mentioned that, because U_f is of order zero and $\partial x/\partial t$ is of second order, the expression $U_f - \partial x/\partial t$ in equation of θ_2 is always positive.

The angles θ_1 and θ_2 may be expressed as

$$\theta_1 = v' - u'v' - \tfrac{1}{3}v'^3 + \mathcal{O}(\varepsilon^5), \tag{25}$$

$$\theta_2 = \frac{\dot{v}}{U_f} + \frac{\dot{x}\dot{v}}{U_f^2} - \tfrac{1}{3}\frac{\dot{v}^3}{U_f^3} + \mathcal{O}(\varepsilon^5), \tag{26}$$

where primes and dots denote derivatives with respect to X and t, respectively. Hence, using series expansions, we can write

$$\begin{aligned} \cos\theta_1 &= 1 - \tfrac{1}{2}v'^2 + \mathcal{O}(\varepsilon^4), \\ \sin\theta_1 &= v' - u'v' - \tfrac{1}{2}v'^3 + \mathcal{O}(\varepsilon^5). \end{aligned} \tag{27}$$

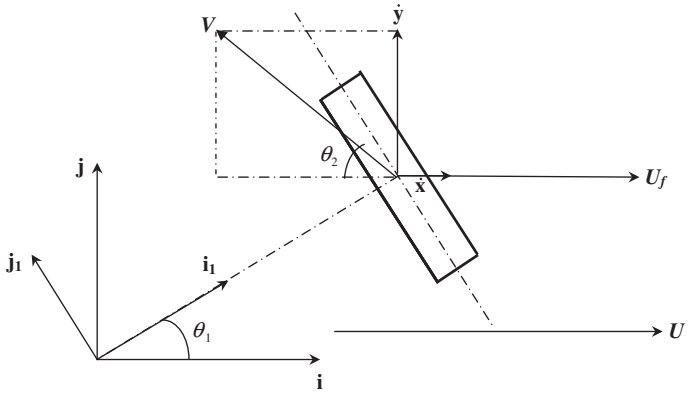

Fig. 3. An element of the cylinder used for the determination of the relative fluid-cylinder velocity V and of the angles θ_1 and θ_2; the latter is the vectorial sum of $\dot{y}$ and $-U_f + \dot{x}$.

Based on Fig. 3, we define the angle of incidence $i = \theta_1 + \theta_2$, which will be used later; it corresponds to the angle between the relative fluid-body velocity and the centreline of the body, so that

$$\cos i = 1 - \frac{1}{2}\left(v'^2 + 2\frac{v'\dot{v}}{U_f} + \frac{\dot{v}^2}{U_f^2}\right) + \mathcal{O}(\varepsilon^4),$$
$$\sin i = v' + \frac{\dot{v}}{U_f} - u'v' + \frac{\dot{u}\dot{v}}{U_f^2} - \frac{1}{2}\left(v'^3 + \frac{\dot{v}^3}{U_f^3} + \frac{v'^2\dot{v}}{U_f} + \frac{v'\dot{v}^2}{U_f^2}\right) + \mathcal{O}(\varepsilon^5). \tag{28}$$

4.2. The inviscid hydrodynamic forces

To determine the inviscid hydrodynamic forces to $\mathcal{O}(\varepsilon^3)$, we adapt Lighthill's work (1960), which is essentially an application of slender body theory [see Lopes et al. (2002) for details].

In Fig. 3, we introduce the new system of unit vectors $(\mathbf{i}_1, \mathbf{j}_1)$, which corresponds to $(\mathbf{i}, \mathbf{j})$ rotated by an angle θ_1 in the counterclockwise direction. We isolate an element of the cylinder as in Fig. 3, and define the relative fluid-body velocity as

$$V = \dot{y} + \dot{x} - U_f. \tag{29}$$

Then, projecting this relative fluid-body velocity on $\mathbf{j}_1$, the direction normal to the element, considering the trigonometric expressions (27), and replacing U_f by U by means of expression (22), the relative fluid-body velocity becomes

$$V(X,t) = \dot{v} + Uv' - \tfrac{1}{2}\dot{v}v'^2 - 2Uu'v' - \tfrac{1}{2}Uv'^3 - \dot{x}v' + \mathcal{O}(\varepsilon^5). \tag{30}$$

The next step involves the extension of Lighthill's linear potential flow theory to a third-order nonlinear formulation, subject to a number of assumptions. Eventually, a nonlinear expression of the lift, is derived, correct to third-order of magnitude (Lopes et al., 2002). The inviscid hydrodynamic force, as used here, has the same magnitude as the lift, but acts in the opposite direction. For a cylinder of constant cross-section, i.e., $(\partial A/\partial X) = 0$ and added mass $M(X) = M = \chi\rho A$, the inviscid hydrodynamic force, may be obtained as

$$F_A(X,T) = \left\{\frac{\partial}{\partial T} + [U(1-u') - (\dot{u} + Uu')]\frac{\partial}{\partial X}\right\} \times \left[V_l - (\dot{u}v' + 2Uu'v') - \frac{1}{2}V_l v'^2\right]M + \frac{1}{2}MV_l v' V_l' + \mathcal{O}(\varepsilon^5), \tag{31}$$

where $V_l = \dot{v} + Uv'$, and therefore

$$F_A(X,T) = M[\ddot{v} - \ddot{u}v' - 2\dot{u}\dot{v}' - \tfrac{1}{2}\ddot{v}v'^2 - \tfrac{3}{2}\dot{v}\dot{v}'v' + U(2\dot{v}' - 3\dot{u}'v' - 4u'\dot{v}' - \tfrac{5}{2}\dot{v}'v'^2 - 2\dot{u}v'' - \tfrac{3}{2}\dot{v}v'v'') + U^2(v'' - 2u''v' - 4u'v'' - 2v'^2v'')] + \mathcal{O}(\varepsilon^5). \tag{32}$$

4.3. The frictional forces

The frictional forces are formulated essentially as proposed by Taylor (1952), i.e.,

$$F_N = \tfrac{1}{2}\rho DU^2(C_N \sin i + C_{Dp}\sin^2 i), \tag{33}$$

$$F_L = \tfrac{1}{2}\rho DU^2 C_T \cos i, \tag{34}$$

respectively, in the normal and longitudinal directions; D is the cylinder diameter, C_{Dp} the form drag coefficient due to the normal component, and C_N and C_T, in general not equal, are the coefficients associated with friction in the normal and tangential directions, respectively.

Combining (33) and (34) with expressions (28) and relating U_f to U through Eq. (22), one obtains

$$F_N = \frac{1}{2}\rho DU^2\left[C_N\left(v' + \frac{\dot{v}}{U} + \frac{\dot{v}u'}{U} - u'v' + \frac{\dot{u}\dot{v}}{U^2} - \frac{1}{2}\left(v'^3 + \frac{\dot{v}^3}{U^3} + \frac{v'^2\dot{v}}{U} + \frac{v'\dot{v}^2}{U^2}\right)\right) + C_{Dp}\left(v'|v'| + \frac{v'|\dot{v}| + |v'|\dot{v}}{U} + \frac{\dot{v}|\dot{v}|}{U^2}\right)\right] + \mathcal{O}(\varepsilon^4), \tag{35}$$

$$F_L = \frac{1}{2}\rho D U^2 C_T \left(1 - \frac{1}{2}\left(v'^2 + 2\frac{v'\dot{v}}{U} + \frac{\dot{v}^2}{U^2}\right)\right) + \mathcal{O}(\varepsilon^4). \tag{36}$$

The quadratic terms in the expression for F_N are modified by using the method proposed by Triantafyllou and Chryssostomidis (1989), in order to obtain forces which are odd with respect to v' and $\dot{v}$, thus forces always opposing motion. In Eqs. (35) and (36), C_N, C_T and C_{Dp} are supposed to be independent of axial location for simplicity.

4.4. The hydrostatic pressure forces

Following the procedure in Lopes et al. (2002), the hydrostatic pressure forces, F_{px} and F_{py} (see Fig. 2), which are the resultants of the steady-state pressure p acting on the outer surface of the element, for a constant cross-section cylinder are found to be

$$-F_{px} = \frac{\partial p}{\partial x} A\left(-\frac{1}{2}v'^2 + u'\right) - v'v''pA + \mathcal{O}(\varepsilon^4), \tag{37}$$

$$F_{py} = \frac{\partial p}{\partial x} A\left(v' - \frac{1}{2}v'^3\right) + pA\left(v'' - u''v' - u'v'' - \frac{3}{2}v'^2v''\right) + \mathcal{O}(\varepsilon^5). \tag{38}$$

Furthermore, by assuming the lateral movement of the cylinder to have a negligible effect on the axial pressure distribution in the fluid at large (its velocity then being U), one may write (Païdoussis, 1973)

$$A\frac{\partial p}{\partial x} = -\frac{1}{2}\rho D U^2 C_T \frac{D}{D_h} + \rho g A, \tag{39}$$

where D is the diameter of the cylinder, D_h is the hydraulic diameter, and C_T is the uniform frictional coefficient, as in Eq. (36).

Knowing that $A(\partial p/\partial X) = A(\partial p/\partial x)(1 + u')$ and using Eq. (39), one can integrate the resulting equation from $X = X$ to L, assuming the cross-sectional area to be constant, and thus obtain

$$Ap(X) = Ap(L) + \left(\frac{1}{2}\rho D U^2 C_T \frac{D}{D_h} - \rho g A\right)\left[L - X + u(L)(1 - \overline{\delta}) - u\right] + \mathcal{O}(\varepsilon^4), \tag{40}$$

where $p(L)$ is the pressure at the downstream end of the cylinder, which may be represented by

$$Ap(L) = \left[(1 - 2\nu)\overline{P}A + \rho g A\frac{L}{2}\right]\overline{\delta}, \tag{41}$$

in which ν is the Poisson ratio; as before $\overline{\delta} = 1$ if there is no sliding at the ends, and $\overline{\delta} = 0$ if the downstream end can slide axially; $\overline{P}$ stands for the value of p at $X = \frac{1}{2}L$.

Combining expression (39) with (37) and (38), we get

$$-F_{px} = \left(-\frac{1}{2}v'^2 + u'\right)\left(-\frac{1}{2}\rho D U^2 C_T \frac{D}{D_h} + \rho g A\right) - v'v''Ap + \mathcal{O}(\varepsilon^4), \tag{42}$$

$$F_{py} = \left(v' - \frac{1}{2}v'^3\right)\left(-\frac{1}{2}\rho D U^2 C_T \frac{D}{D_h} + \rho g A\right) + \left(v'' - u''v' - u'v'' - \frac{3}{2}v'^2v''\right)Ap + \mathcal{O}(\varepsilon^5). \tag{43}$$

4.5. The total virtual work of the fluid forces

The virtual work of these forces on the whole body may be written as

$$\begin{aligned}\int_{t_1}^{t_2} \delta W \, \mathrm{d}t = \int_{t_1}^{t_2}\int_0^L \{&[-F_{Px} + F_L\cos\theta_1 + (F_A + F_N)\sin\theta_1]\,\delta x \\ &+ \left[F_{Py} + F_L\sin\theta_1 - (F_A + F_N)\cos\theta_1\right]\delta y\}\,\mathrm{d}X\,\mathrm{d}t.\end{aligned} \tag{44}$$

One should be very careful when developing expression (44), in the use of the expressions for the forces and trigonometric expressions, Eqs. (27), (32), (35), (36), (42) and (43), to ensure that third-order accuracy is maintained.

For an extensible cylinder, considering two independent variables, one eventually obtains

$$\begin{aligned}\int_{t_1}^{t_2}\delta W\,\mathrm{d}t = &-\int_{t_1}^{t_2}\int_0^L\Bigg\{-\frac{1}{2}\rho DU^2C_T\left(1-\frac{1}{2}\frac{\dot v^2}{U^2}-\frac{\dot v v'}{U}-v'^2\right)-M(\ddot v v'+2U\dot v'v'+U^2v'v'')\\
&-\frac{1}{2}\rho DU^2C_N\left(\frac{\dot v v'}{U}+v'^2\right)-\left(\frac{1}{2}\rho DU^2C_T\frac{D}{D_h}-\rho gA\right)\left(-u'+\frac{1}{2}v'^2-(L-X)v'v''\right)\\
&-\frac{1}{2}\rho DU^2C_{Dp}v'\left(v'|v'|+\frac{v'|\dot v|+\dot v|v'|}{U}+\frac{\dot v|\dot v|}{U^2}\right)+\left[\frac{1}{2}\rho gL\overline{\delta}+(1-2\nu)\overline{p}\right]Av'v''\Bigg\}\,\delta u\,\mathrm{d}X\,\mathrm{d}t\\
&-\int_{t_1}^{t_2}\int_0^L\Bigg\{M\ddot v(1-v'^2)+2MU\dot v'\left(1-\frac{7}{4}v'^2\right)+MU^2v''\left(1-\frac{5}{2}v'^2\right)-Mv'(\ddot u+3U\dot u'+2U^2u'')\\
&-M\left(4Uu'+2\dot u+\frac{3}{2}\dot v v'\right)(\dot v'+Uv'')-\frac{1}{2}\rho DU^2(C_T-C_N)\left(v'-\frac{1}{2}\frac{v'\dot v^2}{U^2}-u'v'-\frac{\dot v v'^2}{U}-v'^3\right)\\
&+\left(\frac{1}{2}\rho DU^2C_T\frac{D}{D_h}-\rho gA\right)\left(v'-\frac{1}{2}v'^3+\left[u-u(L)(1-\overline{\delta})\right]v''-(L-X)\left(v''-u''v'-u'v''-\frac{3}{2}v'^2v''\right)\right)\\
&-\left[\frac{1}{2}\rho gL\overline{\delta}+(1-2\nu)\overline{P}\right]A\left(v''-u''v'-u'v''-\frac{3}{2}v'^2v''\right)\\
&+\frac{1}{2}\rho DU^2C_N\left(\frac{\dot v}{U}+\frac{u'\dot v}{U}+\frac{\dot u\dot v}{U^2}-\frac{1}{2}\frac{\dot v^3}{U^3}\right)\\
&+\frac{1}{2}\rho DU^2C_{Dp}\left(v'|v'|+\frac{v'|\dot v|+\dot v|v'|}{U}+\frac{\dot v|\dot v|}{U^2}\right)\Bigg\}\,\delta v\,\mathrm{d}X\,\mathrm{d}t+\mathcal{O}(\varepsilon^5).\end{aligned}\tag{45}$$

5. Equations of motion

Taking Eqs. (9), (11), (13), (21) and (45) into account, one eventually finds two coupled equations of motion, one in the X- and the other in the Y-direction, describing the behaviour of an extensible cylinder subjected to axial flow:

$$\begin{aligned}&m\ddot u-M(\ddot v v'+2U\dot v'v'+U^2v''v')-EA(u''+v'v'')-EI(v''v'''+v'v'''')\\
&-\frac{1}{2}\rho DU^2(C_N-C_T)\left(\frac{\dot v v'}{U}+v'^2\right)+\frac{1}{4}\rho DC_T\dot v^2+\frac{1}{2}\rho DU^2C_T\left(1+\frac{D}{D_h}\right)\left\{u'-\frac{v'^2}{2}+\left[\left(1-\frac{1}{2}\delta\right)L-X\right]v'v''\right\}\\
&-\frac{1}{2}\rho DU^2C_{Dp}v'\left(v'|v'|+\frac{v'|\dot v|+\dot v|v'|}{U}+\frac{\dot v|\dot v|}{U^2}\right)+\left[\frac{1}{2}\rho D^2U^2C_b(1-\delta)+\overline{T}\delta+(1-2\nu)A\overline{P}\delta\right]v'v''\\
&+(mg-\rho gA)\left\{u'-\frac{v'^2}{2}+\left[\left(1-\frac{1}{2}\delta\right)L-X\right]v'v''\right\}+\mathcal{O}(\varepsilon^5)=0,\end{aligned}\tag{46}$$

$$\begin{aligned}&(m+M)\ddot v+2MU\dot v'\left(1-\frac{7}{4}v'^2\right)+MU^2v''\left(1-\frac{5}{2}v'^2\right)\\
&-Mv'(\ddot u+3U\dot u'+2U^2u'')-M\ddot vv'^2-M\left(4Uu'+2\dot u+\frac{3}{2}\dot v v'\right)(\dot v'+Uv'')\\
&+\left[\frac{1}{2}\rho D^2U^2C_b(1-\delta)+\overline{T}\delta+(1-2\nu)A\overline{P}\delta\right]\left(-v''+v'u''+v''u'+\frac{3}{2}v'^2v''\right)\\
&+\frac{1}{2}\rho DU^2C_{Dp}\left(v'|v'|+\frac{v'|\dot v|+\dot v|v'|}{U}+\frac{\dot v|\dot v|}{U^2}\right)-EA\left(u''v'+u'v''+\frac{3}{2}v'^2v''\right)\\
&+EIv''''-EI(8v'v''v'''+v'u^{(4)}+2v'^2v^{(4)}+2v''^3+2u'v^{(4)}+4u''v'''+3u'''v'')\\
&+\frac{1}{2}\rho DU^2C_T\left(1+\frac{D}{D_h}\right)\left[-\frac{1}{2}v'^3+[u-u(L)(1-\delta)]v''+\left(\left(1-\frac{1}{2}\delta\right)L-X\right)\left(-v''+v'u''+v''u'+\frac{3}{2}v'^2v''\right)\right]\\
&-\frac{1}{2}\rho DU^2(C_N-C_T)\left(v'^3+v'u'+\frac{\dot vv'^2}{U}+\frac{1}{2}\frac{\dot v^2v'}{U^2}\right)+\frac{1}{2}\rho DU^2\left(C_N+C_T\frac{D}{D_h}\right)v'\\
&+\frac{1}{2}\rho DU^2C_N\left(\frac{\dot v}{U}+\frac{u'\dot v}{U}+\frac{\dot u\dot v}{U^2}-\frac{1}{2}\frac{\dot v^3}{U^3}\right)\end{aligned}$$

$$+(mg-\rho gA)\left\{v'-\frac{1}{2}v'^3+[u-u(L)(1-\delta)]v''\right.$$
$$\left.+\left[\left(1-\frac{1}{2}\delta\right)L-X\right]\left(-v''+v'u''+v''u'+\frac{3}{2}v'^2v''\right)\right\}+\mathcal{O}(\varepsilon^5)=0. \tag{47}$$

In Eqs. (46), (47) and what follows, $\bar{\delta}$ has been replaced by δ for simplicity. In order to find the nondimensional form of the equations of motion, we first introduce the following nondimensional quantities:

$$\xi=\frac{X}{L},\quad \zeta=\frac{u}{L},\quad \eta=\frac{v}{L},\quad \tau=\left(\frac{EI}{m+\rho A}\right)^{1/2}\frac{t}{L^2},$$
$$\mathscr{U}=\left(\frac{\rho A}{EI}\right)^{1/2}UL,\quad \beta=\frac{\rho A}{m+\rho A},\quad \gamma=\frac{(m-\rho A)gL^3}{EI},$$
$$c_n=\frac{4}{\pi}C_N,\quad c_t=\frac{4}{\pi}C_T,\quad c_d=\frac{4}{\pi}C_{Dp},\quad c_b=\frac{4}{\pi}C_b,\quad \varepsilon=\frac{L}{D},\quad h=\frac{D}{D_h},$$
$$\overline{\Pi}=\frac{\overline{P}AL^2}{EI},\quad \overline{\Gamma}=\frac{\overline{T}L^2}{EI},\quad \Pi_0=\frac{EAL^2}{EI},\quad \chi=\frac{M}{\rho A}. \tag{48}$$

Next, we replace X, u, v, C_N, C_T and C_{Dp} by their corresponding nondimensional values, ξ, ζ, η, c_n, c_t and c_d, respectively, as defined in (48), to yield the following form for the dimensionless equations:

$$(1-\beta)\ddot{\zeta}-\chi\left(\beta\ddot{\eta}\eta'+2\mathscr{U}\sqrt{\beta}\dot{\eta}'\eta'+\mathscr{U}^2\eta''\eta'\right)-\Pi_0(\zeta''+\eta'\eta'')-(\eta''\eta'''+\eta'\eta^{(4)})$$
$$-\frac{1}{2}\varepsilon\mathscr{U}^2(c_n-c_t)\left(\frac{\sqrt{\beta}}{\mathscr{U}}\dot{\eta}\eta'+\eta'^2\right)+\frac{1}{4}\varepsilon c_t\beta\dot{\eta}^2+\frac{1}{2}\varepsilon\mathscr{U}^2c_t(1+h)\left[\zeta'-\frac{\eta'^2}{2}+\left(1-\frac{1}{2}\delta-\xi\right)\eta'\eta''\right]$$
$$-\frac{1}{2}\varepsilon\mathscr{U}^2c_d\eta'\left(\eta'|\eta'|+\frac{\sqrt{\beta}(\eta'|\dot{\eta}|+\dot{\eta}|\eta'|)}{\mathscr{U}}+\frac{\beta\dot{\eta}|\dot{\eta}|}{\mathscr{U}^2}\right)+\left[\frac{1}{2}\mathscr{U}^2c_b(1-\delta)+\overline{\Gamma}\delta+(1-2v)\overline{\Pi}\delta\right]\eta'\eta''$$
$$+\gamma\left[\zeta'-\frac{\eta'^2}{2}+\left(1-\frac{1}{2}\delta-\xi\right)\eta'\eta''\right]+\mathcal{O}(\varepsilon^5)=0, \tag{49}$$

$$(1+(\chi-1)\beta)\ddot{\eta}+2\chi\mathscr{U}\sqrt{\beta}\dot{\eta}'\left(1-\frac{7}{4}\eta'^2\right)+\chi\mathscr{U}^2\eta''\left(1-\frac{5}{2}\eta'^2\right)-\chi\eta'(\beta\ddot{\zeta}+3\sqrt{\beta}\mathscr{U}\dot{\zeta}'+2\mathscr{U}^2\zeta'')-\chi\beta\ddot{\eta}\eta'^2$$
$$-\chi\left(4\mathscr{U}\zeta'+2\sqrt{\beta}\dot{\zeta}+\frac{3}{2}\sqrt{\beta}\dot{\eta}\eta'\right)\left(\sqrt{\beta}\dot{\eta}'+\mathscr{U}\eta''\right)$$
$$+\left[\frac{1}{2}\mathscr{U}^2c_b(1-\delta)+\overline{\Gamma}\delta+(1-2v)\overline{\Pi}\delta\right]\left(-\eta''+\eta'\zeta''+\eta''\zeta'+\frac{3}{2}\eta'^2\eta''\right)$$
$$+\frac{1}{2}\varepsilon\,\mathscr{U}^2c_d\left(\eta'|\eta'|+\frac{\sqrt{\beta}(\eta'|\dot{\eta}|+\dot{\eta}|\eta'|)}{\mathscr{U}}+\frac{\beta\dot{\eta}|\dot{\eta}|}{\mathscr{U}^2}\right)-\Pi_0\left(\zeta''\eta'+\zeta'\eta''+\frac{3}{2}\eta'^2\eta''\right)$$
$$+\eta^{(4)}-(8\eta'\eta''\eta'''+\eta'\zeta^{(4)}+2\eta'^2\eta^{(4)}+2\eta''^3+2\zeta'\eta^{(4)}+4\zeta''\eta'''+3\zeta'''\eta'')$$
$$+\frac{1}{2}\varepsilon\mathscr{U}^2c_t(1+h)\left(-\frac{1}{2}\eta'^3+[\zeta-\zeta(1)(1-\delta)]\eta''+\left(1-\frac{1}{2}\delta-\xi\right)\left(-\eta''+\eta'\zeta''+\eta''\zeta'+\frac{3}{2}\eta'^2\eta''\right)\right)$$
$$-\frac{1}{2}\varepsilon\mathscr{U}^2(c_n-c_t)\left(\eta'^3+\eta'\zeta'+\beta\frac{\dot{\eta}\eta'^2}{\mathscr{U}}+\frac{1}{2}\beta\frac{\dot{\eta}^2\eta'}{\mathscr{U}^2}\right)+\frac{1}{2}\varepsilon\mathscr{U}^2(c_n+c_th)\eta'$$
$$+\frac{1}{2}\varepsilon\mathscr{U}^2c_n\left(\frac{\sqrt{\beta}}{\mathscr{U}}\dot{\eta}+\frac{\sqrt{\beta}}{\mathscr{U}}\zeta'\dot{\eta}+\frac{\beta}{\mathscr{U}^2}\dot{\zeta}\dot{\eta}-\frac{1}{2}\frac{\beta^{3/2}}{\mathscr{U}^3}\dot{\eta}^3\right)$$
$$+\gamma\left\{\eta'-\frac{1}{2}\eta'^3+[\zeta-\zeta(1)(1-\delta)]\eta''+\left(1-\frac{1}{2}\delta-\xi\right)\left(-\eta''+\eta'\zeta''+\eta''\zeta'+\frac{3}{2}\eta'^2\eta''\right)\right\}+\mathcal{O}(\varepsilon^5)=0. \tag{50}$$

In these equations, ζ and η are, respectively, the dimensionless displacement in the longitudinal and transverse direction; $\mathscr{U}$ is dimensionless flow velocity, used extensively as the independent parameter in studying the dynamics of the system; $\beta=\rho A/(m+\rho A)$ is a mass ratio; $\Pi_0=EAL^2/EI$, $\overline{\Pi}=\overline{P}AL^2/EI$ and $\overline{\Gamma}=\overline{T}L^2/EI$ are dimensionless measures of axial flexibility, pressurization and externally imposed uniform tension, respectively; c_n and c_t are the coefficients of frictional forces in the normal and tangential (longitudinal) directions, respectively; c_d is the coefficient of transverse form drag;

$\delta = 0$ or 1 if the downstream end is free to slide axially (or wholly free), or is axially fixed; v is the Poisson ratio; $\gamma = (m - \rho A)gL^3/EI$ is a gravity coefficient; c_b is the base-drag coefficient acting in the longitudinal direction at the free end of the cylinder when $\delta = 0$; $\varepsilon = L/D$ is the slenderness ratio; $h = D/D_h$ is a hydraulic coefficient, D_h being the hydraulic diameter; and $\chi = M/\rho A$ is an added mass coefficient which increases with increasing confinement.

These equations of motion are valid for all boundary conditions of a slender flexible cylinder subjected to axial flow, either supported at both ends or free at the downstream end.[1] The equation of motion derived in Lopes et al. (2002) is valid only for cantilevered cylinders. In that derivation the inextensibility assumption has been used which relates the displacement in the transverse direction to that in the axial direction, leading to a single equation of motion. In the present equations of motion, however, no such assumption has been made, and hence we have obtained two coupled equations of motion, one mainly for the axial and the other for the transverse direction. In these equations, there are some terms, which would vanish if the inextensibility assumption had been used.[2] There are also some terms in Eqs. (49) and (50) containing external pressure and externally imposed tension on the cylinder, which are not present in the equations of motion for the cantilevered cylinder, because such terms do not exist when there is a free end ($\delta = 0$). There is also a new essential parameter defined in this set of equations, relating the axial and transverse flexibilities of the cylinder (Π_0), which also does not arise if the centreline is inextensible.

6. Method of analysis

As a first step towards solving the partial differential equations of motion, (49) and (50), they are transformed into a set of second-order ordinary differential equations using Galerkin's technique with the beam eigenfunctions $\phi_j(\xi)$ and $\psi_j(\xi)$ used as a suitable set of base functions and with $q_j(\tau)$ and $p_j(\tau)$ the corresponding generalized coordinates; thus

$$\zeta(\xi,\tau) = \sum_{j=1}^{N_u} \psi_j(\xi) p_j(\tau), \tag{51}$$

$$\eta(\xi,\tau) = \sum_{j=1}^{N_v} \phi_j(\xi) q_j(\tau), \tag{52}$$

where N_u and N_v represent the number of modes in the longitudinal and the lateral direction, respectively. Substituting expressions (51) and (52) into (49) and (50), multiplying (49) by $\psi_i(\xi)$ and (50) by $\phi_i(\xi)$ and integrating from 0 to 1, using the fact that $\int_0^1 \psi_i(\xi)\psi_j(\xi)\,\mathrm{d}\xi = \int_0^1 \phi_i(\xi)\phi_j(\xi)\,\mathrm{d}\xi = \delta_{ij}$ (δ_{ij} being the Kronecker delta), leads to the following matrix form:

$$\begin{aligned} &M^u_{ij}\ddot{p}_j + C^u_{ij}\dot{p}_j + K^u_{ij}p_j + A^1_{ijk}q_jq_k + A^2_{ijk}q_j\dot{q}_k + A^3_{ijk}\dot{q}_j\dot{q}_k + A^4_{ijk}q_j\ddot{q}_k \\ &\quad + B^1_{ijkl}q_jq_k|q_l| + B^2_{ijkl}q_j\dot{q}_k|q_l| + B^3_{ijkl}q_jq_k|\dot{q}_l| + B^4_{ijkl}q_j\dot{q}_k|\dot{q}_l| = 0 \end{aligned} \tag{53}$$

and

$$\begin{aligned} &M^v_{ij}\ddot{q}_j + C^v_{ij}\dot{q}_j + K^v_{ij}q_j + D^1_{ijk}p_jq_k + D^2_{ijk}\dot{p}_jq_k + D^3_{ijk}p_j\dot{q}_k + D^4_{ijk}\dot{p}_j\dot{q}_k + D^5_{ijk}\ddot{p}_jq_k + E^1_{ijk}q_j|q_k| + E^2_{ijk}\dot{q}_j|q_k| \\ &\quad + E^3_{ijk}q_j|\dot{q}_k| + E^4_{ijk}\dot{q}_j|\dot{q}_k| + F^1_{ijkl}q_jq_kq_l + F^2_{ijkl}q_jq_k\dot{q}_l + F^3_{ijkl}q_j\dot{q}_k\dot{q}_l + F^4_{ijkl}\dot{q}_j\dot{q}_k\dot{q}_l + F^5_{ijkl}q_jq_k\ddot{q}_l = 0, \end{aligned} \tag{54}$$

where the coefficients are given in the appendix.

Concerning the linear terms, M^u_{ij}, C^u_{ij} and K^u_{ij} correspond, respectively, to the mass, damping and stiffness matrices in the u-direction and M^v_{ij}, C^v_{ij} and K^v_{ij} to the corresponding matrices in the v-direction. All the other terms are related to coefficients of the nonlinear terms in the u and v directions.

In the foregoing, internal dissipation in the material of the cylinder was neglected; for generality, it is now introduced into the equations of motion, via the simplest possible model. The internal dissipation of the cylinder is assumed to be viscous and linear. In order to find the related terms, we look at the linear equations of motion in the axial and the transverse directions, assuming that there are no flow- and gravity-related forces. The linear equations of motion become $M^u_{ij}\ddot{p}_j + K^u_{ij}p_j = 0$ and $M^v_{ij}\ddot{q}_j + K^v_{ij}q_j = 0$, in the axial and the transverse directions, respectively, where $M^u_{ij} = \int_0^1 \psi_i\psi_j\,\mathrm{d}\xi = I_{ij}$, $K^u_{ij} = -\Pi_0\int_0^1 \psi_i\psi_j''\,\mathrm{d}\xi$, $M^v_{ij} = \int_0^1 \phi_i\phi_j\,\mathrm{d}\xi = I_{ij}$, $K^v_{ij} = \int_0^1 \phi_i\phi_j^{(4)}\,\mathrm{d}\xi$; I_{ij} being the identity matrix.

[1] If the end is free, however, special boundary conditions may have to be introduced, to represent the possibly tapering tip of the cylinder (Lopes et al., 2002; Païdoussis, 2003).

[2] Taking the inextensibility assumption into account, one finds $\varepsilon = 0$ in Eq. (2) leading to $\zeta' = -\frac{1}{2}\eta'^2$.

In the axial direction, the linear viscous damping can be written as $C^u_{ij,\text{viscous}} = 2\varsigma(K^u_{ij}M^u_{ij})^{1/2} = 2\varsigma\left(-\Pi_0\int_0^1 \psi_i\psi_j''\,\mathrm{d}\xi\right)^{1/2} = 2\varsigma\sqrt{\Pi_0}\lambda_i^u$; λ_i^u being the ith eigenvalue of a bar in axial vibration, with the same boundary conditions as the cylinder, and ς being the damping ratio. In the same manner, one can find the viscous damping in the transverse direction as $C^v_{ij,\text{viscous}} = 2\varsigma(\lambda_i^v)^2$; λ_i^v being the ith eigenvalue of a beam in transverse vibration. C^u_{ij} and the third term in C^v_{ij} in the appendix are terms associated with this dissipation.

Solutions are obtained by Houbolt's finite difference method (FDM). Houbolt's FDM is an initial-value problem solver in which the system of equations is integrated numerically for one initial condition at a particular time, and the state of the system at any time thereafter can be reproduced (Semler et al., 1996).

7. Analysis of a simply-supported cylinder

In this part of the paper, as an example, the dynamics of a simply-supported cylinder will be studied using the equations presented in the foregoing. In the case of a simply-supported beam, the eigenfunctions of a bar in axial vibration, $\psi_j(\xi)$, and those of a beam in transverse vibration, $\phi_j(\xi)$, are used, which are identical; i.e.,

$$\psi_j(\xi) = \sqrt{2}\sin(j\pi\xi), \tag{55}$$

$$\phi_j(\xi) = \sqrt{2}\sin(j\pi\xi). \tag{56}$$

One can now evaluate the coefficients of the matrix equations in (53) and (54).

Linear analysis of this system (Païdoussis, 1973), considering small motions, can predict the point of first loss of stability, but cannot provide any definitive prediction of its post-critical behaviour. Linear theory predicts that, in general, at low-flow velocities, the cylinder is stable; then, as the flow velocity increases, the cylinder is subjected to divergence (buckling) in its first mode. Linear theory also predicts the occurrence of second-mode buckling of the system, and at higher flow velocities the existence of coupled-mode flutter (so-called "Païdoussis flutter") in some cases. In order to investigate the validity of the post-critical behaviour of the system as predicted by linear theory, and also to determine the amplitude of buckling, as well as the amplitude and frequency of oscillatory motion if flutter does exist, the dynamics needs to be examined via nonlinear analysis.

The information gained from a nonlinear analysis of the system is often summarized in bifurcation diagrams in which, typically, the amplitude of motion is plotted as a function of one parameter of the system; in this paper, the first generalized coordinate of a simply-supported cylinder is plotted as a function of the dimensionless flow velocity. In the bifurcation diagrams, a solution on the x-axis represents the original configuration, i.e., the inert cylinder in its equilibrium position. A nonzero solution can represent either a nontrivial static equilibrium position (representing a buckled stationary cylinder) or the amplitude of oscillation for flutter.

7.1. The influence of different parameters on the stability and the amplitude of the buckled solution

In the following sections, the influence of different parameters on the stability and the amplitude of the buckled solution of the system is examined for the following physical parameters: $D = 0.0254$ m, $\rho = 1000\ \text{kg/m}^3$, $m = 0.5817$ kg/m, $M = 0.507$ kg/m and $E = 2.76$ MPa; leading to the following dimensionless values: $\mathscr{U} \simeq 3UL$, $\beta = 0.47$, $\gamma = 12.996L^3$ and $\tau = 0.27t/L^2$, where U is in m/s, L in m and t in s. Here $\mathscr{U}$ is used as the independent parameter, which is varied. It is assumed that $\chi = 1$ and $h = 0$, which corresponds to a cylinder in unconfined flow, and that the coefficient of form drag is zero, $c_d = 0$. The cylinder is not allowed to slide at the downstream end; hence, $\delta = 1$ and $c_b = 0$. The damping ratio, ς, is assumed to be 0.01 in all modes.

7.1.1. Influence of frictional coefficients

In this study, the frictional coefficients in the normal and tangential directions are assumed to be equal, $c_n = c_t$ (Païdoussis, 2003, Appendix Q). Also, since in the equations of motion they always appear as εc_n and εc_t, the effect of varying $\varepsilon c_n = \varepsilon c_t$ is the same as varying $c_n = c_t$. Fig. 4(a) shows the bifurcation diagram of the system for different values of $\varepsilon c_n = \varepsilon c_t$. Here it is assumed that $\Pi_0 = 10\,000$, corresponding to $L = 64$ cm and $\varepsilon = 25$, and $\bar{\Gamma} = 0$. It is seen that, with increasing εc_n and εc_t, the first bifurcation point (divergence) occurs at progressively lower flow velocities; also at a fixed flow velocity, the amplitude of buckling is increased with larger values of these coefficients. These two effects could be explained by noting that larger εc_n and εc_t imply that half the cylinder is subjected to an increasing compressive load.

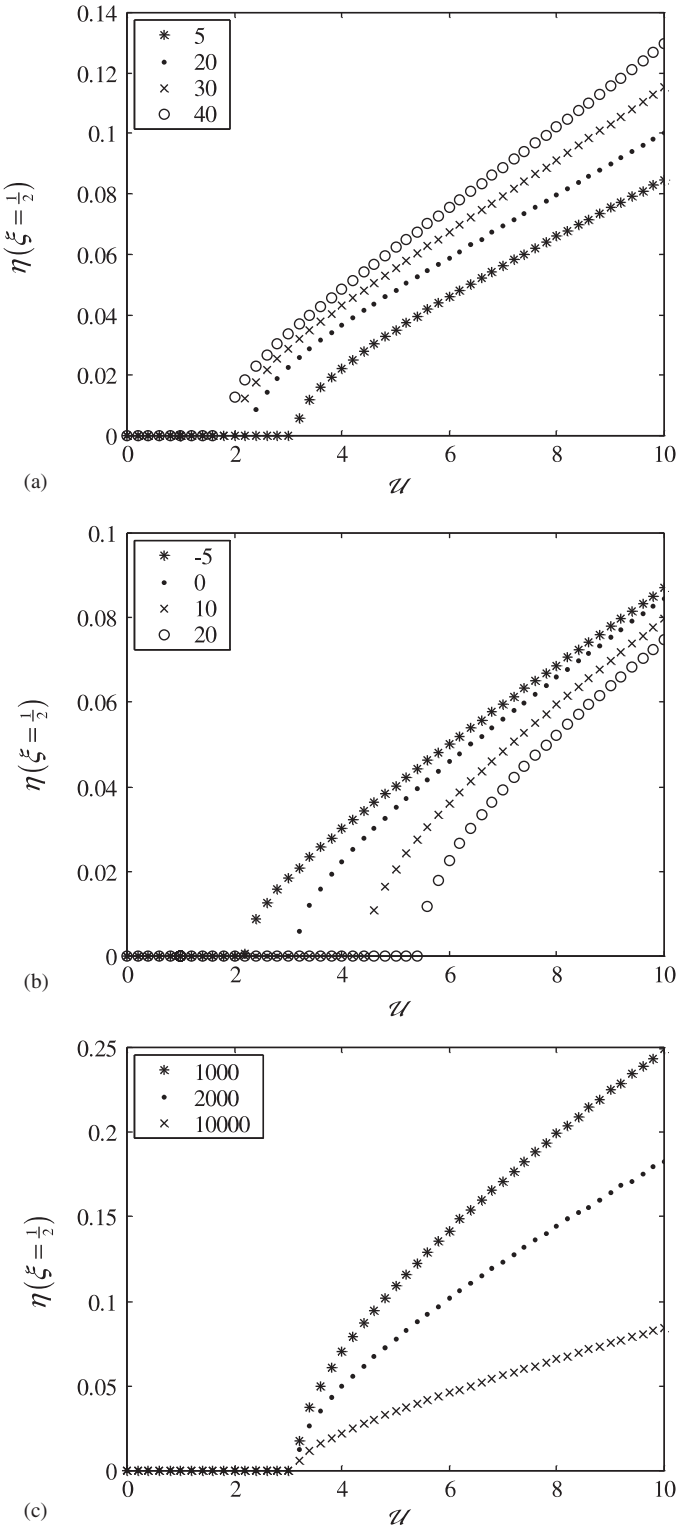

Fig. 4. Bifurcation diagrams of a simply-supported cylinder obtained with $N_u = N_v = 2$ and with (a) different values of $\varepsilon c_n = \varepsilon c_t$, ranging from 5 to 40, (b) different values of $\overline{\Gamma}$, ranging from –5 to 20, and (c) different values of Π_0, ranging from 1000 to 10 000.

7.1.2. Influence of externally imposed uniform tension

An externally imposed uniform tension ($\overline{\Gamma} = \overline{T}L^2/EI$) represents a pre-strain in the longitudinal direction of the cylinder. Fig. 4(b) shows the bifurcation diagrams of the system with varying $\overline{\Gamma}$ for $\Pi_0 = 10\,000$ and $c_n = c_t = 0.025$. When a larger tension is applied on a cylinder, higher flow velocities are needed to cause instability; hence, the critical flow velocity (for divergence) increases. With increasing $\overline{\Gamma}$ at a fixed flow velocity, the amplitude of bucking decreases. This is because in a stretched cylinder, the lateral displacement will be reduced. One would expect the same influence on the behaviour of the system for the coefficient of base drag (c_b) and pressurization ($\overline{\Pi}$), both of them representing a pre-strain in the longitudinal direction of the cylinder.

7.1.3. Influence of dimensionless axial flexibility

The dimensionless axial flexibility $\Pi_0 = EAL^2/EI$ is a measure of the axial rigidity as compared with the transverse rigidity of the system. For a full cylinder (not hollow), $\Pi_0 = (4L/D)^2$; this implies that, for a fixed D, increasing the value of Π_0 means a larger L; therefore, a larger amplitude of buckling should be expected. Fig. 4(c) shows the bifurcation diagrams of the system for different values of Π_0 for $c_n = c_t = 0.025$ and $\overline{\Gamma} = 0$. It is seen that, the larger the value of Π_0 is, the *smaller* the amplitude of buckling becomes! The answer to this paradox lies in the fact that the dimensionless flow velocity and the dimensionless transverse displacement, both depend on the length of the cylinder. Once this is taken into account, the results are as one would expect. It has also to be noticed that Π_0 has no influence on the first bifurcation point.

7.2. On nonlinear post-divergence behaviour of the system

Fig. 5 shows a bifurcation diagram for a simply-supported cylinder with the parameters mentioned in Section 7.1. This bifurcation diagram is for $\Pi_0 = 4000$, corresponding to $L = 40$ cm and therefore $\varepsilon = 15.81$; it is also assumed that $c_n = c_t = 0.025$ and $\overline{\Gamma} = 0$. As is well known, bifurcations are determined mathematically by the eigenvalues in the case of a fixed point, and by the Floquet multipliers in the case of a periodic solution. A complete description may be found in Païdoussis (1998). Fig. 5 has been obtained using six modes (in the Galerkin solution) each in the axial and the transverse directions. The first generalized coordinate, q_1, is representative of the behaviour of the system.

As expected, the system is stable at very low flow velocities corresponding to the original equilibrium state, up to where it loses stability via a supercritical pitchfork bifurcation (one eigenvalue is equal to zero) at a nondimensional flow velocity $\mathscr{U} \simeq \pi$ in conformity with linear theory, and it leads to divergence (stable nonzero static solution or fixed point). Subsequently, q_1 increases with $\mathscr{U}$. The resulting static solution eventually loses stability, and the system develops flutter via a supercritical Hopf bifurcation (two complex-conjugate eigenvalues with zero real parts) at $\mathscr{U} \simeq 14.23$, corresponding to periodic solutions around the buckled positions (fixed points). Figs. 6(a)–(c) show the time history, phase-plane and power-spectral-density plots of the periodic response of the system at $\mathscr{U} = 14.6$, where the system is subject to flutter. The system oscillates around the static equilibrium point, where $q_1 \simeq 0.082$.

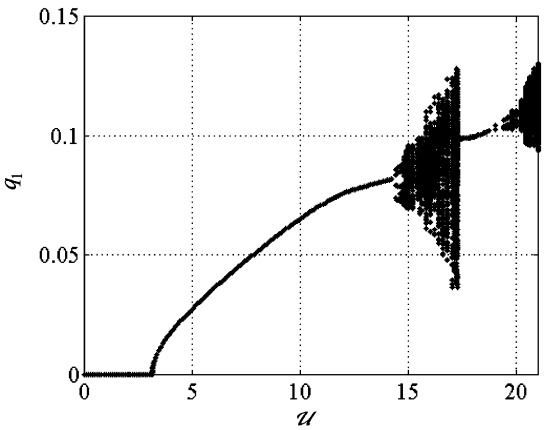

Fig. 5. Bifurcation diagram of a simply-supported cylinder with $\beta = 0.47, \gamma = 0.838, c_n = c_t = 0.025$, $\varepsilon = 15.81$, $\delta = 1, \nu = 0.47$, $\Pi_0 = 4000$, $\chi = 1, \overline{\Pi} = \overline{\Gamma} = c_b = c_d = 0$, obtained with $N_u = N_v = 6$.

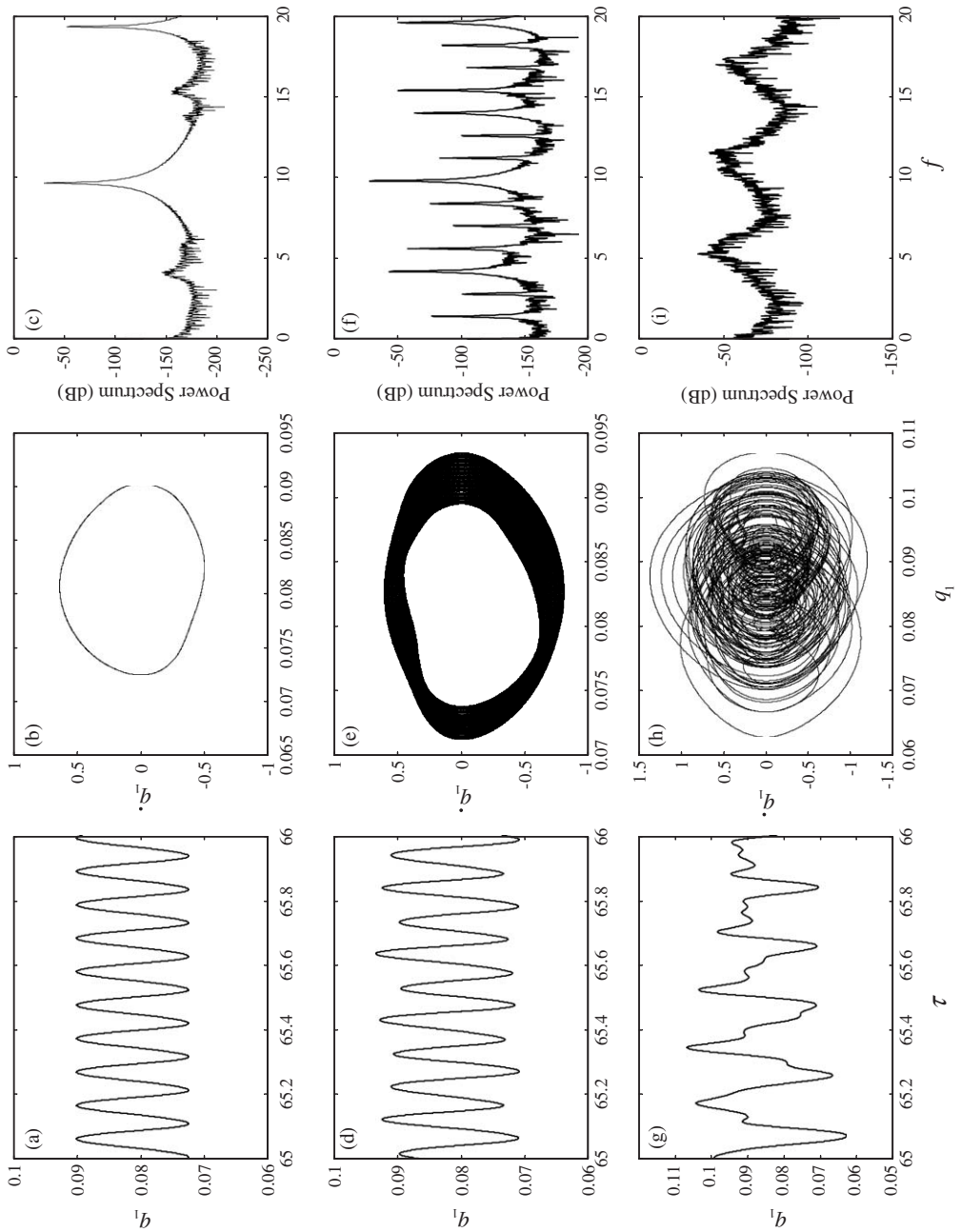

Fig. 6. Time histories, phase plane plots and power spectral density plots for the system of Fig. 5 for different flow velocities: $\mathscr{U} = 14.6$ (first row of diagrams); $\mathscr{U} = 14.8$ (second row) and $\mathscr{U} = 16$ (third row), obtained with $N_u = N_v = 6$.

Table 1
Flow velocity at which the first Hopf bifurcation (HB) occurs versus the number of modes in the two directions used in the computations

$N_u = N_v$	4	5	6	7	8
Value of first HB flow velocity	14.3123	14.7772	14.2334	14.1557	14.1110

The resulting limit cycle then becomes unstable via a torus bifurcation (two complex-conjugate Floquet multipliers cross the unit circle) at $\mathscr{U} \simeq 14.73$. This bifurcation usually corresponds to the appearance of a second frequency in the periodic response, indicating that quasiperiodic solutions are possible thereafter. Figs. 6(d)–(f) show the time history, phase-plane and power-spectral-density plots of the system at $\mathscr{U} = 14.8$, which indicates a quasiperiodic-two oscillation, as it involves two fundamental frequencies. The two dominant frequencies are $f_1 = 1.4114$ and $f_2 = 2.7847$, so that all the other peaks in the PSD may be confirmed to correspond to $f = mf_1 \pm nf_2$ with m and n integers. The time history, phase-plane and power-spectral-density plots of the system at $\mathscr{U} = 16$ are shown in Figs. 6(g)–(i). The oscillation here is chaotic. In the PSD, chaotic oscillations are associated with a wide frequency band. At $\mathscr{U} = 16$, notice that, although the main frequency and its harmonics are still very prominent, the subharmonic content is fundamentally flat and quite high.

At higher flow velocities, there is a range of flow velocities (between $\mathscr{U} = 16.9$ and $\mathscr{U} = 17.25$) in which two different attractors co-exist: a nonzero static attractor and a chaotic (strange) attractor.[3] The static branch loses its stability by a Hopf bifurcation at $\mathscr{U} = 18.73$ and a periodic motion arises with a relatively high frequency (around 30 Hz). This high-frequency periodic motion becomes unstable via a torus at $\mathscr{U} = 19.6$ leading to a quasiperiodic motion.

The dynamics of this system has been studied, using two modes in each direction by Modarres-Sadeghi et al. (2003). It was also shown that if one imposes a very large initial value for the first generalized coordinate, a large-amplitude high-frequency flutter-like motion of the cylinder is predicted; this unrealistic motion disappears when the number of transverse-direction modes used in the solution is increased sufficiently, as done here.

As Table 1 shows, the flow velocity at which the first Hopf bifurcation occurs, converges to $\mathscr{U} = 14.2$–14.1 for $N_u = N_v = 6$ and greater. Using$N_u = N_v = 7$, the system has been found to behave similarly to the case of six modes in each direction, both qualitatively and quantitatively. The only difference is that the periodic solution of the system becomes unstable via a period-doubling bifurcation at $\mathscr{U} = 14.53$ (one of the Floquet multipliers crosses the unit circle at –1) followed by a torus at $\mathscr{U} = 14.73$, which corresponds to the critical value for the torus bifurcation, found when using six modes in each direction.

8. Conclusion

In this paper, a weakly nonlinear equation of motion, correct to third-order of magnitude, has been derived for the dynamics of an extensible slender cylinder subjected to axial flow using Hamilton's principle. Here, lateral deflections are assumed to be of first-order magnitude, while axial ones of second order. For convenience, inviscid, hydrostatic and viscous forces are determined separately, not together, say by direct application of the Navier–Stokes equations. This equation is probably not the definitive nonlinear equation of motion for this system, since it was not obtained by a unified nonlinear treatment of the fluid mechanics.

Based on the derived nonlinear equations of motion, the dynamics of the system was studied from a nonlinear point of view, and the existence of post-divergence instabilities of the cylinder was proved, in qualitative agreement with observation (Païdoussis, 1966b). Also, the effect of some of the key parameters affecting the critical flow velocities and the amplitude of the resultant motions were explored. It is found that the system loses stability by a pitchfork bifurcation leading to divergence, and the new equilibrium at higher flow becomes unstable by a Hopf bifurcation, leading to flutter. With further increases in the flow velocity, the dynamics becomes more complex, and quasiperiodic and chaotic solutions have been obtained.

[3]The static deformation of the cylinder (static solution) at $\mathscr{U} = 18$ was calculated. Surprisingly perhaps, it is basically of first-mode shape, albeit with strong second-mode and substantial third-mode contributions. In contrast, close to the onset of divergence, i.e., at $\mathscr{U} = \pi$, the deformation is nearly a half sinusoid (the classical first-mode shape).

Acknowledgement

Support of this research by NSERC of Canada and FCAR of Québec is gratefully acknowledged.

Appendix

The coefficients of the matrix form of the equations of motion (53) and (54), are given here, as follows[4,5]:

$$M^u_{ij} = (1-\beta)\int_0^1 \psi_i\psi_j \,\mathrm{d}\xi, \quad C^u_{ij} = 2\varsigma\lambda^u_i\sqrt{\Pi_0},$$

$$K^u_{ij} = -\Pi_0\int_0^1 \psi_i\psi_j'' \,\mathrm{d}\xi + \left[\frac{1}{2}U^2\varepsilon c_t(1+h)+\gamma\right]\int_0^1 \psi_i\psi_j' \,\mathrm{d}\xi,$$

$$\begin{aligned} A^1_{ijk} = & -\left(\frac{1}{2}\gamma+\frac{1}{2}U^2\varepsilon\left(c_n+\frac{1}{2}(h-1)c_t\right)\right)\int_0^1 \psi_i\phi_j'\phi_k' \,\mathrm{d}\xi \\ & +\left(\gamma\left(1-\frac{1}{2}\delta\right)-U^2\chi+(1-2v)\overline{\Pi}\delta\right. \\ & \left.+\overline{\Gamma}\delta+\frac{1}{2}U^2c_b(1-\delta)+\frac{1}{2}U^2\varepsilon c_t(1+h)\left(1-\frac{1}{2}\delta\right)-\Pi_0\right)\int_0^1 \psi_i\phi_j'\phi_k'' \,\mathrm{d}\xi \\ & -\left(\gamma+\frac{1}{2}U^2\varepsilon c_t(1+h)\right)\int_0^1 \xi\psi_i\phi_j'\phi_k'' \,\mathrm{d}\xi - \int_0^1 \psi_i\phi_j'\phi_k'' \,\mathrm{d}\xi - \int_0^1 \psi_i\phi_j'\phi_k^{(4)} \,\mathrm{d}\xi, \end{aligned}$$

$$A^2_{ijk} = \frac{1}{2}U\sqrt{\beta}\varepsilon(c_t-c_n)\int_0^1 \psi_i\phi_j'\phi_k \,\mathrm{d}\xi - 2\chi U\sqrt{\beta}\int_0^1 \psi_i\phi_j'\phi_k' \,\mathrm{d}\xi,$$

$$A^3_{ijk} = \frac{1}{4}\beta\varepsilon c_t\int_0^1 \psi_i\phi_j\phi_k \,\mathrm{d}\xi, \quad A^4_{ijk} = -\chi\beta\int_0^1 \psi_i\phi_k'\phi_k \,\mathrm{d}\xi,$$

$$B^1_{ijkl} = -\frac{1}{2}U^2\varepsilon c_d\int_0^1 \psi_i\phi_j'\phi_k'|\phi_l'| \,\mathrm{d}\xi, \quad B^2_{ijkl} = -\frac{1}{2}U\sqrt{\beta}\varepsilon c_d\int_0^1 \psi_i\phi_j'\phi_k|\phi_l'| \,\mathrm{d}\xi,$$

$$B^3_{ijkl} = -\frac{1}{2}U\sqrt{\beta}\varepsilon c_d\int_0^1 \psi_i\phi_j'\phi_k'|\phi_l| \,\mathrm{d}\xi, \quad B^4_{ijkl} = -\frac{1}{2}\beta\varepsilon c_d\int_0^1 \psi_i\phi_j'\phi_k|\phi_l| \,\mathrm{d}\xi;$$

$$M^v_{ij} = (1+(\chi-1)\beta)\int_0^1 \phi_i\phi_j \,\mathrm{d}\xi,$$

$$C^v_{ij} = \frac{1}{2}U\varepsilon c_n\sqrt{\beta}\int_0^1 \phi_i\phi_j \,\mathrm{d}\xi + 2\chi U\sqrt{\beta}\int_0^1 \phi_i\phi_j' \,\mathrm{d}\xi + 2\varsigma(\lambda^v_i)^2,$$

$$\begin{aligned} K^v_{ij} = & \left(\gamma+\frac{1}{2}U^2\varepsilon(c_n+hc_t)\right)\int_0^1 \phi_i\phi_j' \,\mathrm{d}\xi - \left(\gamma\left(1-\frac{1}{2}\delta\right)-U^2\chi+(1-2v)\overline{\Pi}\delta+\overline{\Gamma}\delta\right. \\ & \left.+\frac{1}{2}U^2c_b(1-\delta)+\frac{1}{2}U^2\varepsilon c_t(1+h)\left(1-\frac{1}{2}\delta\right)\right)\int_0^1 \phi_i\phi_j'' \,\mathrm{d}\xi \\ & +\left(\gamma+\frac{1}{2}U^2\varepsilon c_t(1+h)\right)\int_0^1 \xi\phi_i\phi_j'' \,\mathrm{d}\xi + \int_0^1 \phi_i\phi_j^{(4)} \,\mathrm{d}\xi, \end{aligned}$$

[4]Here, λ^u_i is the ith eigenvalue of a bar in axial vibration and ς is the damping ratio.
[5]λ^v_i is the ith eigenvalue of a beam in transverse vibration.

$$
\begin{aligned}
D^1_{ijk} = {} & \left(\gamma + \frac{1}{2}U^2\varepsilon c_t(1+h)\right)\int_0^1 \phi_i\psi_j\phi_k'' \,\mathrm{d}\xi + \left(\gamma\left(1-\frac{1}{2}\delta\right) - 2U^2\chi + (1-2\nu)\overline{\Pi}\delta + \overline{\Gamma}\delta\right.\\
& \left. + \frac{1}{2}U^2 c_b(1-\delta) + \frac{1}{2}U^2\varepsilon c_t(1+h)\left(1-\frac{1}{2}\delta\right) - \Pi_0\right)\int_0^1 \phi_i\psi_j''\phi_k' \,\mathrm{d}\xi\\
& - \left(\gamma + \frac{1}{2}U^2\varepsilon c_t(1+h)\right)\int_0^1 \xi\phi_i\psi_j''\phi_k' \,\mathrm{d}\xi - \frac{1}{2}U^2\varepsilon(c_n - c_\mathrm{t})\int_0^1 \phi_i\psi_j'\phi_k' \,\mathrm{d}\xi\\
& + \left(\gamma\left(1-\frac{1}{2}\delta\right) - 4U^2\chi + (1-2\nu)\overline{\Pi}\delta + \overline{\Gamma}\delta\right.\\
& \left. + \frac{1}{2}U^2 c_b(1-\delta) + \frac{1}{2}U^2\varepsilon c_t(1+h)\left(1-\frac{1}{2}\delta\right) - \Pi_0\right)\int_0^1 \phi_i\psi_j'\phi_k'' \,\mathrm{d}\xi\\
& - \left[\gamma + \frac{1}{2}U^2\varepsilon c_t(1+h)\right]\int_0^1 \xi\phi_i\psi_j'\phi_k'' d\xi - \left[\gamma + \frac{1}{2}U^2\varepsilon c_t(1+h)\right](1+\delta)\int_0^1 \phi_i\psi_j(1)\phi_k'' \,\mathrm{d}\xi\\
& - 4\int_0^1 \phi_i\psi_j''\phi_k''' \,\mathrm{d}\xi - 3\int_0^1 \phi_i\psi_j'''\phi_k'' d\xi - 2\int_0^1 \phi_i\psi_j'\phi_k^{(4)} \,\mathrm{d}\xi - \int_0^1 \phi_i\psi_j^{(4)}\phi_k' \,\mathrm{d}\xi,
\end{aligned}
$$

$$
D^2_{ijk} = -\chi U\sqrt{\beta}\left(3\int_0^1 \phi_i\psi_j'\phi_k' \,\mathrm{d}\xi + 2\int_0^1 \phi_i\psi_j\phi_k'' \,\mathrm{d}\xi\right),
$$

$$
D^3_{ijk} = \frac{1}{2}U\sqrt{\beta}\varepsilon c_n\int_0^1 \phi_i\psi_j'\phi_k \,\mathrm{d}\xi - 4\chi U\sqrt{\beta}\int_0^1 \phi_i\psi_j'\phi_k' \,\mathrm{d}\xi,
$$

$$
D^4_{ijk} = \frac{1}{2}\beta\varepsilon c_n\int_0^1 \phi_i\psi_j\phi_k \,\mathrm{d}\xi - 2\chi\beta\int_0^1 \phi_i\psi_j\phi_k' \,\mathrm{d}\xi, \quad D^5_{ijk} = -\chi\beta\int_0^1 \phi_i\psi_j\phi_k' \,\mathrm{d}\xi,
$$

$$
E^1_{ijk} = \frac{1}{2}U^2\varepsilon c_d\int_0^1 \phi_i\phi_j'|\phi_k'| \,\mathrm{d}\xi, \quad E^2_{ijk} = \frac{1}{2}U\sqrt{\beta}\varepsilon c_d\int_0^1 \phi_i\phi_j|\phi_k'| \,\mathrm{d}\xi,
$$

$$
E^3_{ijk} = \frac{1}{2}U\sqrt{\beta}\varepsilon c_d\int_0^1 \phi_i\phi_j'|\phi_k| \,\mathrm{d}\xi, \quad E^4_{ijk} = \frac{1}{2}\beta\varepsilon c_d\int_0^1 \phi_i\phi_j|\phi_k| \,\mathrm{d}\xi,
$$

$$
\begin{aligned}
F^1_{ijkl} = {} & -\frac{1}{2}\left(\gamma + U^2\varepsilon\left(c_n + \frac{1}{2}c_t(h-1)\right)\right)\int_0^1 \phi_i\phi_j'\phi_k'\phi_l' \,\mathrm{d}\xi\\
& + \left(\frac{3}{2}\gamma\left(1-\frac{1}{2}\delta\right) - \frac{5}{2}U^2\chi + \frac{3}{2}(1-2\nu)\overline{\Pi}\delta + \frac{3}{2}\overline{\Gamma}\delta\right.\\
& \left. + \frac{3}{4}U^2 c_b(1-\delta) + \frac{3}{4}U^2\varepsilon c_t(1+h)\left(1-\frac{1}{2}\delta\right) - \frac{3}{2}\Pi_0\right)\int_0^1 \phi_i\phi_j'\phi_k'\phi_l'' \,\mathrm{d}\xi\\
& - \left(\frac{3}{2}\gamma + \frac{3}{4}U^2\varepsilon c_t(1+h)\right)\int_0^1 \xi\phi_i\phi_j'\phi_k'\phi_l'' \,\mathrm{d}\xi\\
& - 2\int_0^1 \phi_i\phi_j'\phi_k'\phi_l^{(4)} \,\mathrm{d}\xi - 8\int_0^1 \phi_i\phi_j'\phi_k''\phi_l''' \,\mathrm{d}\xi - 2\int_0^1 \phi_i\phi_j''\phi_k''\phi_l'' \,\mathrm{d}\xi,
\end{aligned}
$$

$$
F^2_{ijkl} = \frac{1}{2}U\varepsilon\beta(c_t - c_n)\int_0^1 \phi_i\phi_j'\phi_k'\phi_l \,\mathrm{d}\xi - \chi U\sqrt{\beta}\left(\frac{7}{2}\int_0^1 \phi_i\phi_j'\phi_k'\phi_l' \,\mathrm{d}\xi + \frac{3}{2}\int_0^1 \phi_i\phi_j'\phi_k''\phi_l \,\mathrm{d}\xi\right),
$$

$$
F^3_{ijkl} = \frac{1}{4}\beta\varepsilon(c_t - c_n)\int_0^1 \phi_i\phi_j'\phi_k\phi_l \,\mathrm{d}\xi - \frac{3}{2}\chi\beta\int_0^1 \phi_i\phi_j'\phi_k\phi_l' \,\mathrm{d}\xi,
$$

$$
F^4_{ijkl} = -\frac{1}{4}\frac{\beta^{3/2}\varepsilon c_n}{U}\int_0^1 \phi_i\phi_j\phi_k\phi_l \,\mathrm{d}\xi, \quad F^5_{ijkl} = -\chi\beta\int_0^1 \phi_i\phi_j'\phi_k'\phi_l \,\mathrm{d}\xi.
$$

References

Chen, S.S., 1975. Vibration of nuclear fuel bundles. Nuclear Engineering and Design 35, 399–422.

Dowling, A.P., 1998a, b. The dynamics of the towed flexible cylinders. Part 1: neutrally buoyant elements, Part 2: negatively buoyant elements. Journal of Fluid Mechanics 187, 507–532, 533–571.

Hawthorne, W.R., 1961. The early development of the Dracone flexible barge. Proceedings of the Institution of Mechanical Engineers 175, 52–83.

Lighthill, M.J., 1960. Note on the swimming of slender fish. Journal of Fluid Mechanics 9, 305–317.

Lopes, J.L., Païdoussis, M.P., Semler, C., 2002. Linear and nonlinear dynamics of cantilevered cylinders in axial flow. Part 2: the equation of motion. Journal of Fluids and Structures 16, 715–737.

Modarres-Sadeghi, Y., Païdoussis, M.P., Semler C., Picot, P., 2003. Nonlinear dynamics of slender cylinders supported at both ends and subjected to axial flow. IUTAM Symposium on Fluid–Structure Interactions, Rutgers University, USA, Paper T05.

Mote Jr., C.D., 1968. Dynamic stability of an axially moving band. Journal of the Franklin Institute 285, 329–346.

Païdoussis, M.P., 1966a, b. Dynamics of flexible slender cylinders in axial flow. Part 1: theory, Part 2: experiments. Journal of Fluid Mechanics 26, 717–736, 737–751.

Païdoussis, M.P., 1968. Stability of towed, totally submerged flexible cylinders. Journal of Fluid Mechanics 34, 273–297.

Païdoussis, M.P., 1970. Dynamics of submerged towed cylinders. Eighth Symposium on Naval Hydrodynamics: Hydrodynamics in the Ocean Environment, United States ONR, ARC-179, pp. 981–1016.

Païdoussis, M.P., 1973. Dynamics of cylindrical structures subjected to axial flow. Journal of Sound and Vibration 29, 365–385.

Païdoussis, M.P., 1998. Fluid–Structure Interactions: Slender Structures and Axial Flow, vol. 1. Academic Press, London.

Païdoussis, M.P., 2003. Fluid–Structure Interactions: Slender Structures and Axial Flow, vol. 2. Elsevier Academic Press, London.

Païdoussis, M.P., Suss, S., 1977. Stability of a cluster of flexible cylinders in bounded flow. Journal of Applied Mechanics 44, 401–408 (Discussion, 1978, vol. 45, pp. 455, 703).

Païdoussis, M.P., Mateescu, D., Sim, W.-G., 1990. Dynamics and stability of a flexible cylinder in a narrow coaxial cylindrical duct subjected to annular flow. Journal of Applied Mechanics 57, 232–240.

Païdoussis, M.P., Grinevich, E., Adamovic, D., Semler, C., 2002. Linear and nonlinear dynamics of cantilevered cylinders in axial flow. Part 1: physical dynamics. Journal of Fluids and Structures 16, 691–713.

Pramila, A., 1987. Natural frequencies of a submerged axially moving band. Journal of Sound and Vibration 113, 198–203.

Semler, C., Gentleman, W.C., Païdoussis, M.P., 1996. Numerical solutions of second-order implicit ordinary differential equations. Journal of Sound and Vibration 195, 553–574.

Semler, C., Lopes, J.-L., Augu, N., Païdoussis, M.P., 2002. Linear and nonlinear dynamics of cantilevered cylinders in axial flow. Part 3: nonlinear dynamics. Journal of Fluids and Structures 16, 739–759.

Stoker, J.J., 1968. Nonlinear Elasticity. Gordon and Breach, New York.

Taylor, G.I., 1952. Analysis of the swimming of long and narrow animals. Proceedings of the Royal Society (London) A 214, 158–183.

Triantafyllou, G.S., Chryssostomidis, C., 1985. Stability of a string in axial flow. ASME Journal of Energy Resources Technology 107, 421–425.

Triantafyllou, G.S., Chryssostomidis, C., 1989. The dynamics of towed arrays. ASME Journal of Offshore Mechanics and Arctic Engineering 111, 208–213.